Int. J. Solids Structures Vol. 22, No. 8, pp. 909–917, 1986
Printed in Great Britain.

0020-7683/86 $3.00 + .00
Pergamon Journals Ltd.

ELECTRICALLY EXCITABLE MECHANICAL RESONANT MODE SHAPES IN THE ELECTRO-OPTIC CERAMIC PLZT7/65/35

PETER J. CHEN
Sandia National Laboratories, Albuquerque, NM 87185, U.S.A.

(*Received* 23 *April* 1985)

Abstract—In this article we present results concerning electrically excitable mechanical resonant mode shapes of a virgin disc specimen of the electro-optic ceramic PLZT7/65/35. The measurements are made with a dual-beam displacement laser interferometer system capable of determining simultaneously the displacements of opposite points of the surfaces of the disc. It is shown that mechanical resonances with only nodal rings are resonances in the classical sense, whereas those with nodal diameters (nodal rings may or may not be present) are not. The quadrature components of the displacements of the latter exhibit mode shapes as predicted within the framework of the theory of linear elasticity, but their in-phase components exhibit mode shapes having entirely disparative features. In particular, the nodal diameters are not diameters with zero displacements.

1. INTRODUCTION

In a previous article, we have announced the existence of a new electromechanical coupling phenomenon in the electro-optic ceramic PLZT7/65/35[1]. Specifically, when a low amplitude d.c. voltage is applied across a *virgin* disc specimen of the ceramic, the specimen displaces in the direction opposite to the positive direction of the voltage with no measurable accompanying axial strain. Along any diameter of the disc, the displacement profile is "parabolic". This observation is entirely symmetrical in that it remains valid when the polarity of the applied voltage is switched. This coupling phenomenon also manifests itself when a.c. voltages are applied. In which case, the vibrational patterns of the disc depend on the frequencies of the driving voltage. Details of the nonresonant vibrational patterns are given in the paper by Chen[1].

The disc specimen also exhibits resonant modes at particular frequencies. It is our intent to present in this article the details of these resonant modes. It is shown that those resonant modes with *only* nodal rings are completely consistent with the structural resonances as predicted within the framework of the classical theory of linear elasticity. While the frequencies of those with nodal diameters agree with the predictions of this theory, these modes are not resonant modes in the classical sense in that the phase angles between the measured displacements and the driving voltage are not uniform over the surfaces of the disc. The measured displacements have both quadrature and in-phase components. The quadrature components exhibit the mode shapes as predicted by classical theory. The in-phase components are present everywhere, including the nodal diameters. Therefore, the nodal diameters are not diameters with zero displacement.

2. EXPERIMENTAL DETAILS

The displacements of the disc surfaces are measured with the aid of a dual-beam laser interferometer developed at Sandia National Laboratories. This interferometer is actually two modified displacement interferometers with a single He–Ne light source. Each of the interferometers has a quadrature leg so that the direction of motion can also be determined. The signal beams of the interferometers are perpendicularly directed at the opposite surfaces of the specimen. Careful alignment of the signal beams ensures that we can indeed measure the displacements of *opposite* points of the surfaces. Rotation and translation of the specimen with respect to the signal beams thus permit us to determine its vibrational mode shapes.

The virgin PLZT7/65/35 disc specimen of interest has a diameter of 2.342×10^{-2} m and a thickness of 2.616×10^{-4} m. Its average grain size is 4.1×10^{-6} m, and its surfaces are highly polished. The center circular regions of the surfaces of diameter 1.648×10^{-2} m are electroded with vapor-deposited aluminum of thickness 3×10^{-7} m. The specimen is gently held at its edge in the vertical plane by three symmetrically located small sponges within a rather massive annulus. The base on which the annulus rests may be translated. In effect, the specimen may be rotated and translated with respect to the two signal beams of the dual-beam laser interferometer.

The electroded areas of the specimen are, of course, highly reflective. Because the specimen is highly polished, the unelectroded regions are also reflective. The fringe intensity as measured in these regions is approximately a third of that in the electroded regions. Electrical contact with the specimen is effected with the use of 1×10^{-4}-m gold wires attached to the electroded regions with tiny drops of silver paint. The specimen is also connected in series with an integrating capacitor whose capacitance is large compared to that of the specimen. This permits the determination of the electrical charge.

During the course of the experiment we measure the voltage corresponding to the amplitude of a full interference fringe, the voltage corresponding to the interference fringe due to the displacement of a surface point, and the phase angle between the fringe voltage of the displacement and the applied voltage. These measurements are taken for selected points of each surface of the specimen. We also measure the amplitude of the voltage across the integrating capacitor, and the phase angle between this voltage and the applied voltage.

Since each degree of the interference fringe corresponds to 8.7889×10^{-10} m, the amplitude u_0 of the displacement is given by

$$u_0 = \sin^{-1}(V_m/V_f) \times 8.7889 \times 10^{-10}\,\text{m},$$

where V_m is the fringe voltage amplitude of the displacement, and V_f is the fringe voltage amplitude of a full interference fringe. This formula is valid when the fringe voltage amplitude of the displacement is less than that of a full interference fringe. The resolution of this measurement is of order 2.5×10^{-10} m.

The amplitude Q_0 of the charge Q on the integrating capacitor is given by

$$Q_0 = CV_{C0},$$

where C is its capacitance, and V_{C0} is the amplitude of the voltage across it. The current I in the circuit is given by $\dot{Q}$.

The applied alternating voltage V may be represented by

$$V = V_0 \sin \omega t,$$

where V_0 is its amplitude, ω its frequency, and t the time. The displacement u is, therefore,

$$\begin{aligned} u &= u_0 \sin(\omega t + \phi_u) \\ &= u_0 \sin \omega t \cos \phi_u + u_0 \cos \omega t \sin \phi_u, \end{aligned}$$

where ϕ_u is the phase angle between the displacement and the applied voltage. Clearly, the in phase component u_I is given by

$$u_I = u_0 \sin \omega t \cos \phi_u,$$

and the quadrature component u_Q is given by

$$u_Q = u_0 \cos \omega t \sin \phi_u.$$

In a similar vein, the charge is given by

$$Q = Q_0 \sin(\omega t + \phi_Q),$$

where ϕ_Q is the phase angle between the charge and the applied voltage.

Therefore, the in-phase component Q_I is

$$Q_I = Q_0 \sin \omega t \cos \phi_Q,$$

and the quadrature component Q_Q is

$$Q_Q = Q_0 \cos \omega t \sin \phi_Q.$$

Since ϕ_u is a local measurement for each point of each surface of the specimen, the specimen is said to exhibit a *mechanical resonance* if and only if

$$\phi_u = n\pi/2, \qquad n = 1, 3, 5, \ldots,$$

everywhere. Namely, the in-phase component of the displacement vanishes everywhere on the surfaces of the specimen. This corresponds to the classical definition of a mechanical resonance. On the other hand, ϕ_Q is a global measurement, therefore, an electrical resonance is said to exist if and only if

$$\phi_Q = n\pi/2, \qquad n = 1, 3, 5, \ldots.$$

3. EXPERIMENTAL RESULTS AND DISCUSSIONS

Generally speaking, the existence of a resonance at a particular frequency is established when the fringe voltage signal of the displacement and the driving voltage are in quadrature. The Lissajous display of the fringe voltage (y-axis) versus the driving voltage (x-axis) is, therefore, a circle or an ellipse depending on the scales.† Resonances with only nodal rings are readily established because the quadrature condition is satisfied everywhere on both surfaces of the specimen. These resonances are resonances in the classical sense.

Resonances with nodal diameters (nodal rings may or may not be present depending on the frequencies) are not resonances in the classical sense. This is because the fringe voltage signal of the displacement and the driving voltage are not in quadrature everywhere on either surface of the specimen. Therefore, the measured displacement exhibits both quadrature and in-phase components. Resonant frequencies are, therefore, those frequencies at which the quadrature components have relative maximum magnitudes without regard to the values of the resulting phase angle ϕ_u. Once a resonant frequency has been established at a particular point on the specimen surface, the quadrature components also have relative maximum magnitudes for all other points. Hence there is no ambiguity as to the frequencies of these resonances.

It is of importance to note that for the mechanical resonances which we have determined there are no detectable changes in the phase angle ϕ_Q between the charge and the driving voltage. In particular, these mechanical resonances are not accompanied by any electrical

† Cf. Chen[2, 3].

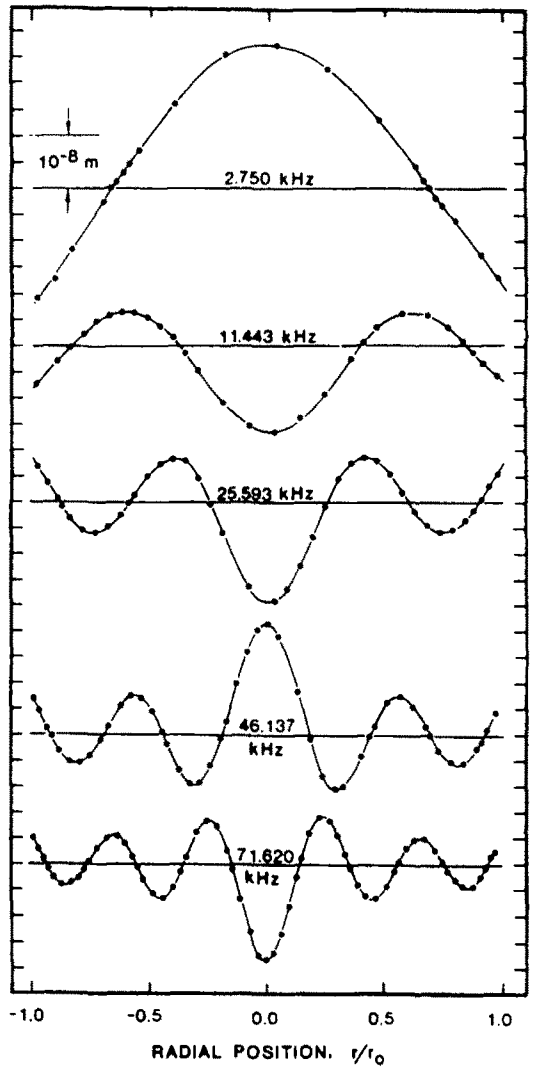

Fig. 1. Displacements of resonant mode shapes with only nodal rings. Amplitudes of driving voltage are 0.25 V for $j = 1$, 0.75 V for $j = 2$, 5.0 V for $j = 3$ and $j = 4$, and 10 V for $j = 5$.

resonance. The lowest detectable electrical resonance of an identical but poled specimen occurs at 89.75 kHz.

In Fig. 1 we exhibit the five resonant mode shapes with only nodal rings. In particular, we plot the amplitudes of the quadrature components, viz.

$$u_{Q0} = u_0 \sin \phi_u,$$

at

$$\omega t = 2n\pi, \qquad n = 0, 1, 2, \ldots .$$

Let i denote the number of nodal diameters, and j denote the number of nodal rings. The ratios of the radii r of the nodal rings to the disc radius a as determined experimentally are

	j				
	1	2	3	4	5
r/a	0.675	0.387 0.838	0.252 0.590 0.894	0.184 0.439 0.692 0.921	0.144 0.349 0.554 0.756 0.935

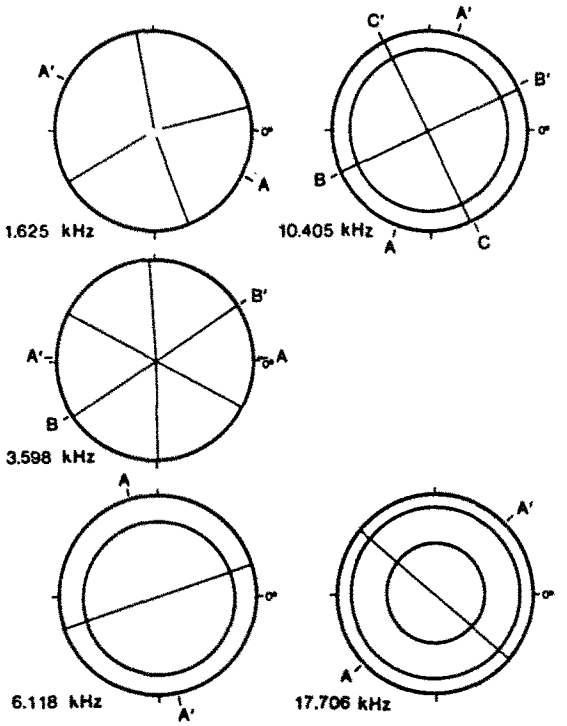

Fig. 2. Plan view of the locations of nodal diameters and nodal rings relative to 0° reference exhibited by the quadrature components of resonant mode shapes with nodal diameters.

These results are in excellent agreement with those (for $j \leqslant 3$) as predicted within the framework of the theory of linear elasticity (see, e.g. p. 240 of Blevins[4] for a disc with free edge). Blevins also gives a formula for the frequencies of these resonant modes. If we normalize the calculated frequency of the $i = 0, j = 1$ mode to the measured frequency, we find that

j	Measured kHz	Calculated kHz
1	2.75	2.75
2	11.443	11.67
3	25.953	26.58

These results are also in excellent agreement.

We now consider those resonances with nodal diameters. Again, normalizing the calculated frequency of the $i = 0, j = 1$ mode to the measured frequency, we have

i	j	Measured kHz	Calculated kHz
2	0	1.625	1.59
3	0	3.598	3.70
1	1	6.118	6.21
2	1	10.405	10.67
3	1	15.632	16.02
1	2	17.706	18.12
2	2	24.872	25.40

In Fig. 2 we exhibit the locations of the nodal diameters and nodal rings of five of these modes as determined experimentally.† Notice that the nodal diameters of the $i = 2, j = 0$

† We identified the existence of $i = 3, j = 1$ and $i = 2, j = 2$ modes. No detailed data of these resonances were taken.

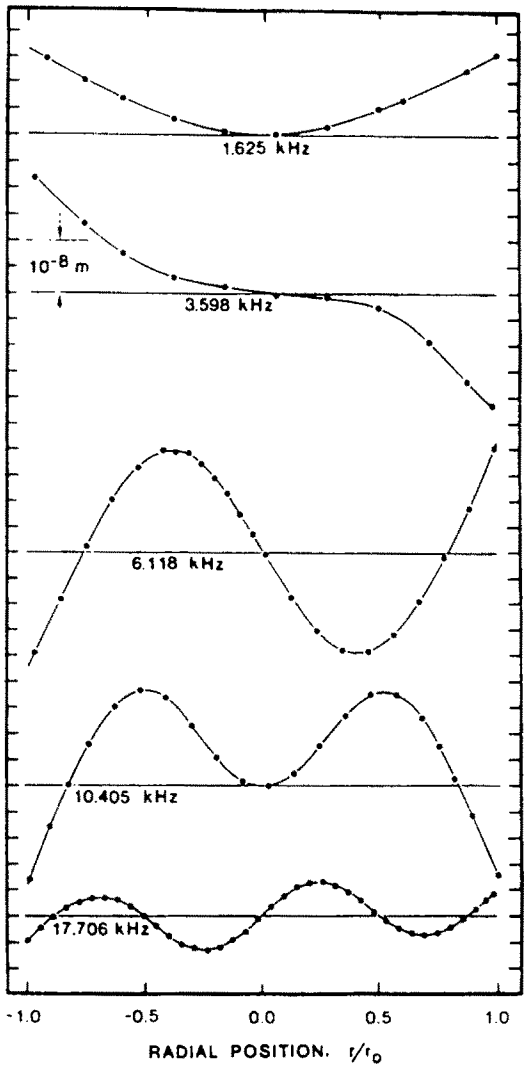

Fig. 3. Quadrature components of displacements along $A-A'$ (see Fig. 2). Amplitudes of driving voltage are 10.0 V.

and $i = 3, j = 0$ modes are not precisely nodal diameters, but rather nodal radii. This may be due to the sponge mountings of the specimen. The symmetry of the nodal diameters are much better at the higher frequency resonant modes.

Figure 3 shows the amplitudes u_{Q0} of the quadrature components at $\omega t = 2n\pi$, $n = 0, 1, 2, \ldots$ along the diameter $A-A'$ of each resonant mode. The amplitudes u_{I0} of the in-phase components are given by

$$u_{I0} = u_0 \cos \phi_u.$$

Hence the values of u_{I0} are very sensitive to the values of ϕ_u when these values are in the neighborhoods of $n\pi/2, n = 1, 3, 5, \ldots$. For the $i = 1, j = 1$ and $i = 1, j = 2$ modes, we are not able to obtain consistent and accurate data of ϕ_u when its values are in the neighborhoods of $n\pi/2, n = 1, 3, 5, \ldots$. This may be due to the inherent instabilities of the modes. Nevertheless, the results which we wish to illustrate are exemplified by the data of the three remaining modes. In Fig. 4 we exhibit the amplitudes u_{I0} of the in-phase components along $A-A'$ of these modes at $\omega t = n\pi/2, n = 1, 5, 9, \ldots$. These results indicate that the amplitudes of the in-phase components of these modes are quite large.

In order to illustrate that the in-phase components of these modes are present everywhere, we compare the amplitudes u_{I0} along $A-A'$ with those along the nodal diameter

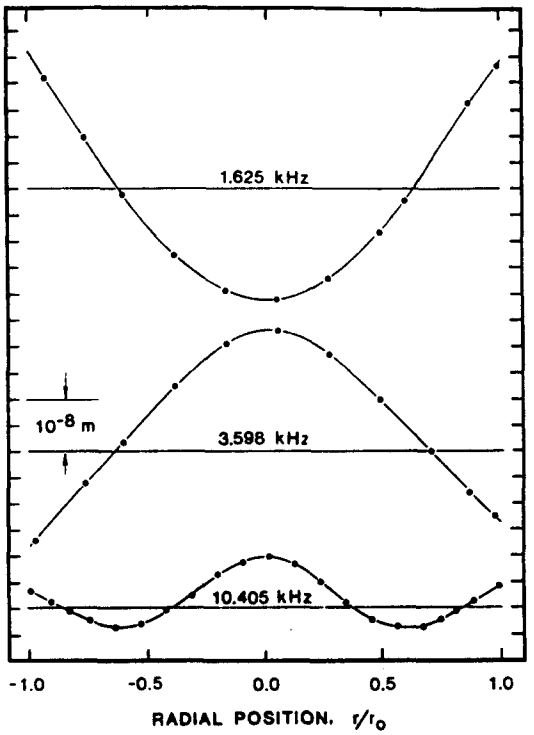

Fig. 4. In-phase components of displacements along $A-A'$ (see Fig. 2). Amplitudes of driving voltage are 10.0 V.

$B-B'$ for the $i=3, j=0$ mode in Fig. 5, and the amplitudes u_{I0} along $A-A'$ with those along the nodal diameters $B-B'$ and $C-C'$ for the $i=2, j=1$ mode in Fig. 6.

Finally, we illustrate in Fig. 7 for the $i=2, j=1$ mode the contours of constant amplitudes of the displacements u_0 and the quadrature components u_{Q0}. The contours of the in-phase components are concentric rings. The contours of displacements are what would be observed with dust pattern and holographic techniques, provided sufficient contrasts can be attained. Notice that they exhibit eight nodal points. Clearly, data concerning the phase angle ϕ_u are required to resolve the displacements into their quadrature and in-phase components in order to ascertain the nature of the resonant modes with nodal diameters.

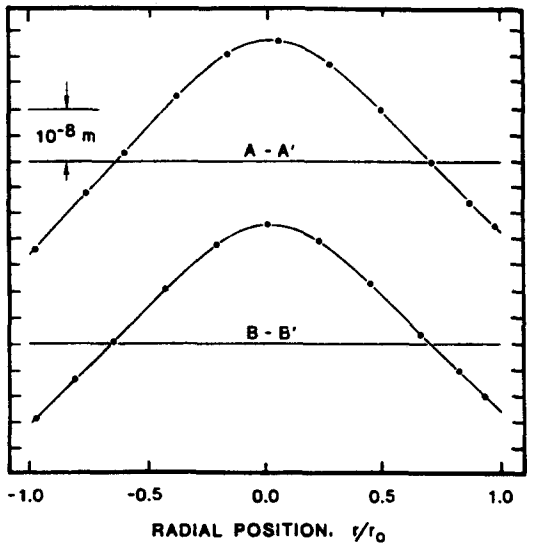

Fig. 5. Comparison of in-phase components of displacements along $A-A'$ and $B-B'$ for $i=3$, $j=0$ mode.

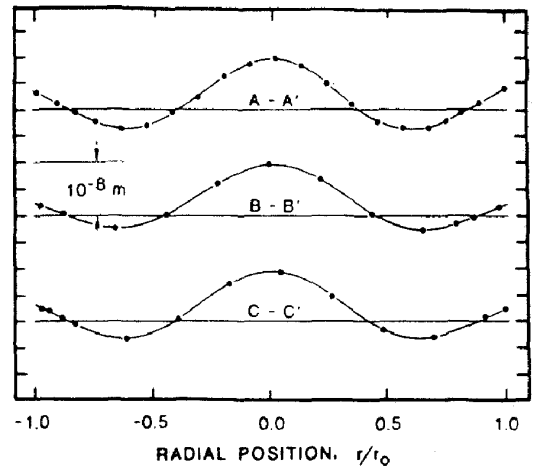

Fig. 6. Comparison of in-phase components of displacements along $A-A'$, $B-B'$ and $C-C'$ for $i=2$, $j=1$ mode.

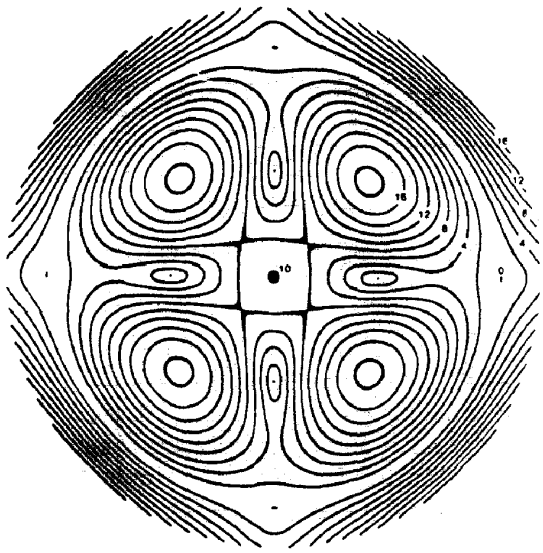

CONTOURS OF DISPLACEMENTS

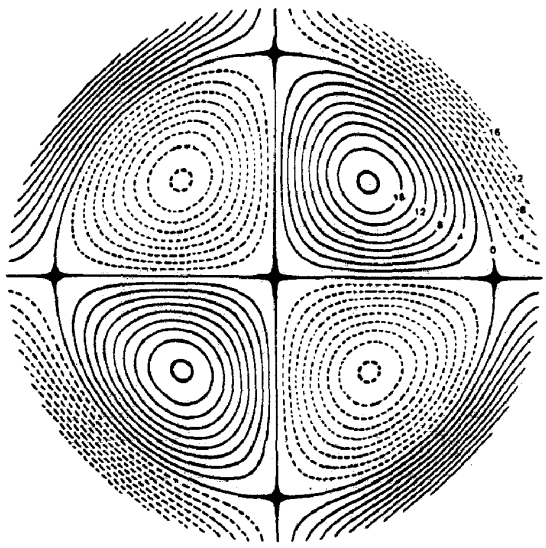

CONTOURS OF QUADRATURE COMPONENTS

Fig. 7. Contours of displacements and quadrature components of displacements of $i=2$, $j=1$ mode. Contours of in-phase components of displacements are concentric rings. The units of the contours are 10^{-9} m.

Acknowledgement—The continuing assistance of Dwight L. Allensworth is gratefully acknowledged. This work performed at Sandia National Laboratories was supported by the U.S. Department of Energy under contract number DE-AC04-DP00789.

REFERENCES

1. P. J. Chen, A new electromechanical coupling phenomenon in the electrooptic ceramic PLZT7/65/35. *Il Nuovo Cimento* **4D**, 280–292 (1984).
2. P. J. Chen, Observation of the existence of electrically excited purely mechanical resonance in piezoelectric and ferroelectric materials. *Il Nuovo Cimento* **2D**, 1145–1155 (1983).
3. P. J. Chen, Electrically excitable purely mechanical resonances in piezoelectric and ferroelectric materials—geometrical considerations. *Wave Motions* **5**, 177–183 (1983).
4. R. D. Blevins, *Formulas for Natural Frequency and Mode Shape*. Van Nostrand Reinhold, New York (1979).